Direct and indirect measurement of the magnetocaloric effect in $La_{0.67}Ca_{0.33-x}Sr_xMnO_{3 \pm \delta}$ ($x \in [0; 0.33]$)

2005 J. Phys.: Condens. Matter 17 6257

(http://iopscience.iop.org/0953-8984/17/39/011)

INSTITUTE OF PHYSICS PUBLISHING JOURNAL OF PHYSICS: CONDENSED MATTER

J. Phys.: Condens. Matter **17** (2005) 6257–6269 doi:10.1088/0953-8984/17/39/011

Direct and indirect measurement of the magnetocaloric effect in $La_{0.67}Ca_{0.33-x}Sr_xMnO_{3\pm\delta}$ ($x \in [0; 0.33]$)

A R Dinesen[1], S Linderoth[1,3] and S Mørup[2]

[1] Materials Research Department, Risø National Laboratory, Frederiksborgvej 399, DK-4000 Roskilde, Denmark
[2] Department of Physics, Technical University of Denmark, DK-2800 Kongens Lyngby, Denmark

E-mail: soren.linderoth@risoe.dk

Received 4 July 2005
Published 16 September 2005
Online at stacks.iop.org/JPhysCM/17/6257

Abstract

The magnetocaloric properties of a series of manganites with the composition $La_{0.67}Ca_{0.33-x}Sr_xMnO_{3\pm\delta}$, $x \in [0; 0.33]$ (LCSM), have been investigated by direct and indirect measuring techniques. The compounds showed a magnetocaloric effect near the Curie temperature, which increased from 267 K for $x = 0$ to 369 K for $x = 0.33$. Both the adiabatic temperature change and the isothermal magnetic entropy change were found to decrease upon increased replacement of Ca with Sr, in good agreement with previous reports. However, all samples showed almost the same relative cooling power, RCP, because the decrease in maximum magnetocaloric effect was accompanied by a widening of the magnetocaloric peaks. The compounds showed RCP values of about 300 mJ cm^{-3} upon a field change of 1.2 T, which is about three times less than the RCP of gadolinium, the prototype material for magnetic cooling at ambient conditions. However, the LCSM materials show a magnetocaloric effect in temperature ranges where the magnetocaloric effect in pure Gd is vanishing. LCSM might therefore have potential as a working substance in multi-component refrigerant units, where the possibility of tailoring compounds with a specific magnetic transition temperature is essential.

(Some figures in this article are in colour only in the electronic version)

1. Introduction

Magnetic refrigeration near room temperature is an interesting alternative to conventional vapour compression-based refrigeration because magnetic cooling technology may be friendlier to the environment—as regards both energy consumption and emission of substances

[3] Author to whom any correspondence should be addressed.

considered harmful to the environment [1]. Magnetic refrigeration is therefore a candidate for commercial and industrial use, such as in air-conditioning systems and refrigerators. The most essential part of a magnetic refrigerator unit is the solid refrigerant—a magnetic solid, which exhibits a magnetocaloric effect, i.e. its temperature changes upon change of the external magnetic field. The magnetic refrigerator utilizes the magnetocaloric effect and takes the refrigerant through a heat pump cycle. The cooling apparatus can be designed in various ways and several proof-of-principle devices have already been constructed to demonstrate magnetic refrigeration near room temperature in the laboratory [2–5]. In most of these devices, the refrigerant consisted of gadolinium (Gd). Gd shows a substantial magnetocaloric effect near its Curie temperature (∼293 K) [1, 5], and it is considered a prototype material for magnetic refrigeration at room temperature. Other refrigerant candidates are lanthanide-based alloys, such as $Gd_5(Si_2Ge_2)$, known as giant magnetocaloric effect (GME) materials [6], Fe_2P-based alloys such as $MnFeP_{1-x}As_x$ [7], Fe-based intermetallics, e.g. $La(Fe_{0.98}Co_{0.02})_{11.7}Al_{1.3}$ [8], and some perovskite-type ceramics, for instance doped manganites of the type $R_xA_{1-x}MnO_3$, where R = rare earth cation, e.g. La^{3+}, Y^{3+}, Pr^{3+}, . . .; A = divalent alkali ion, e.g. Ca^{2+}, Sr^{2+}, Ba^{2+}, and $x \approx 0.2$–0.33. The discovery by Morelli *et al* [9] that manganites exhibiting so-called colossal magnetoresistance (CMR) may also show a significant magnetocaloric effect near room temperature has prompted substantial interest in the magnetocaloric properties of this group of materials. Several reports on the magnetic entropy change in manganites with various compositions have been presented; see e.g. [10–14]. A few investigations involving measurements of both the entropy change and the adiabatic temperature change in manganites have also been performed (e.g. [15–17]).

Below we present results of an investigation on the magnetocaloric effect in a series of manganite compounds belonging to the family $La_{0.67}Ca_{0.33-x}Sr_xMnO_{3\pm\delta}$ (LCSM) with $x \in [0; 0.33]$. It has previously been demonstrated [18] that these compounds show quite large isothermal magnetic entropy changes, $\Delta S_M(T)_{\Delta H}$, near their Curie temperature, which increases from ∼260 to ∼370 K when x is varied from 0 to 0.33. In this study the LCSM series was revisited and, in addition to indirect measurements of the magnetic entropy changes, the investigation involved direct measurement of adiabatic temperature changes, $\Delta T_{ad}(T)_{\Delta H}$. Combining $\Delta S_M(T)_{\Delta H}$ data with zero-field heat capacity measurements, theoretical values for $\Delta T_{ad}(T)_{\Delta H}$ were derived. Calculated and observed temperature changes were found to be in good agreement. The replacement of Ca with Sr in the LCSM series caused a reduction of both $\Delta S_M(T)_{\Delta H}$ and $\Delta T_{ad}(T)_{\Delta H}$. The decrease in magnetocaloric effect coincided with an orthorhombic-to-rhombohedral phase transition. As previously suggested by other authors [12, 18], the large magnetocaloric effects in the orthorhombic LCSM phases are due to an abrupt change of the lattice parameters at the Curie temperature, which contributes to the change of the magnetization. The dynamic Jahn–Teller effect, which causes the volume change, is not present in the compounds with rhombohedral symmetry, which therefore shows a lower magnetocaloric effect.

It has been pointed out [19] that the magnetocaloric effect in manganites, which are often claimed to be competitive with gadolinium, is in fact inferior to that of the prototype material. It is common to exclusively compare the isothermal magnetic entropy change and not take into account that manganites, due to their quite large heat capacity, cannot compete with Gd as regards the adiabatic temperature change. With this in mind, we still found it worthwhile to study manganites as a possible alternative to Gd because they, in contrast to Gd, can be used for cooling at temperatures above 300 K. Furthermore, they are potentially cheaper than Gd, and they do not suffer from corrosion. Having measurements of both the isothermal magnetic entropy change and the adiabatic temperature change enables us to make a reasonable comparison with Gd.

2. Theoretical remarks

According to classical thermodynamics and the thermodynamic Maxwell equation, the isothermal magnetic entropy change, $\Delta S_{\mathrm{M}}(T)_{\Delta H}$, of a spin system upon a change of the magnetic field strength, $\Delta H = H_{\mathrm{F}} - H_{\mathrm{I}}$, from an initial value H_{I} to a final value H_{F} is given by [1]

$$\Delta S_{\mathrm{M}}(T)_{\Delta H} = \mu_0 \int_{H_{\mathrm{I}}}^{H_{\mathrm{F}}} \left(\frac{\partial \sigma}{\partial T}\right)_{\mathrm{H}} \mathrm{d}H, \tag{1}$$

where T is the temperature, μ_0 the permeability of free space, and σ the specific magnetization. The temperature and field dependence of the entropy change can be derived from a series of isothermal magnetization measurements performed at discrete temperatures and fields using a numerical approximation to equation (1) [1]. The magnetic entropy change characterizes the cooling capacity, q, of the material, i.e. the amount of heat that can be transferred from the cold end at temperature T_{L} to the hot end at temperature T_{H} in one ideal thermodynamic cycle [1]:

$$q = \int_{T_{\mathrm{L}}}^{T_{\mathrm{H}}} \Delta S_{\mathrm{M}}(T)_{\Delta H} \, \mathrm{d}T. \tag{2}$$

The temperature change $\Delta T_{\mathrm{ad}}(T)_{\Delta H}$ due to a change of the external magnetic field, also called the adiabatic temperature change, is given as [1]

$$\Delta T_{\mathrm{ad}}(T)_{\Delta H} = -\mu_0 \int_{H_{\mathrm{I}}}^{H_{\mathrm{F}}} \frac{T}{C_P} \left(\frac{\partial \sigma}{\partial T}\right)_{\mathrm{H}} \mathrm{d}H, \tag{3}$$

where C_P is the heat capacity at constant pressure P. When comparing different magnetocaloric materials it is useful to calculate the relative cooling power (RCP) based on the magnetic entropy change and the adiabatic temperature change, defined as [1]

$$\mathrm{RCP}(S) = |\Delta S_{\mathrm{M}}(\max)| \times W(\Delta S_{\mathrm{M}}), \tag{4}$$

and

$$\mathrm{RCP}(T) = \Delta T_{\mathrm{ad}}(\max) \times W(\Delta T_{\mathrm{ad}}), \tag{5}$$

where W denotes the full width at half-maximum. Below, we use measured zero-field heat capacities and magnetic entropy changes to calculate theoretical values for the adiabatic temperature change, which we then compare with directly measured $\Delta T_{\mathrm{ad}}(T)_{\Delta H}$ values. We first calculate the total entropy, $S_{\mathrm{tot}}(T)$, from the heat capacity data using that [20]

$$S_{\mathrm{tot}}(T) = \int_0^T \frac{C_P}{T'} \mathrm{d}T' + S_0, \tag{6}$$

where S_0 is the entropy at zero temperature. We take $S_0 = 0$ and evaluate equation (6) by numerical integration [20, 21]. Because of the lack of data for heat capacity between $T = 0$ K and the first measuring temperature, T_1, we use the Debye model for the lattice heat capacity [5], assuming that this the dominating heat capacity contribution at low temperatures, and calculate the total entropy at T_1 using

$$S_{\mathrm{tot}}(T_1) = \int_0^{T_1} \frac{C_{\mathrm{L}}}{T'} \mathrm{d}T' + S_0,$$

with

$$C_{\mathrm{L}}(T) = 9 n_{\mathrm{a}} k_{\mathrm{B}} \left(\frac{T}{\Theta_{\mathrm{D}}}\right)^3 \int_0^{\Theta_{\mathrm{D}}/T} \frac{x^4 \mathrm{e}^x}{(\mathrm{e}^x - 1)^2} \mathrm{d}x, \tag{7}$$

where n_a is the number of atoms per unit mass and Θ_D is the Debye temperature. We calculate n_a from the nominal sample compositions and take Θ_D to vary linearly between 430 K for $x = 0$ and 385 K for $x = 0.33$ (values obtained from the literature [22, 23]). Having calculated the total entropy in zero field it is straightforward to calculate the entropy in a field $H = H_F$ using experimental values for the magnetic entropy change [20]:

$$S_{tot}(T)_H = S_{tot}(T)_{H=0} - |\Delta S_M(T)_{\Delta H=H_F}|. \tag{8}$$

The entropy–temperature (S–T) diagram with isofield curves for $H = 0$ and H_F has now been generated. From this diagram $\Delta T_{ad}(T)_{\Delta H}$ values can be extracted as the isentropic distance between the two curves.

3. Experimental details

Seven polycrystalline $La_{0.67}Ca_{0.33-x}Sr_xMnO_{3\pm\delta}$ samples with target compositions given by $x = 0$, 0.055, 0.110, 0.165, 0.220, 0.275, and 0.330 were prepared by the glycine–nitrate synthesis technique [24]. Aqueous solutions of pro analysis grade $La(NO_3)_3{\cdot}4H_2O$, $Ca(NO_3)_2{\cdot}4H_2O$, $Sr(NO_3)_2{\cdot}H_2O$, and $Mn(NO_3){\cdot}4H_2O$ were mixed in appropriate ratios. Glycine was added to the solutions and fine-grained LCSM powders were produced by glycine–nitrate combustion. The powders were calcined in air for 5 h at 1375 K and subsequently pressed into pellets, which were sintered in air for 5 h at 1775 K. The chemical composition of the samples was investigated by energy dispersive x-ray spectroscopy (EDS) using a scanning electron microscope (JEOL-840) equipped with a Noran x-ray detector. The actual compositions were found to be in rather good agreement with the nominal compositions, although the EDS technique could not be used to properly determine the oxygen stoichiometry. Exact values of δ therefore remain uncertain.

Structural characterization was carried out by means of x-ray diffraction at room temperature utilizing a Bragg–Brentano set-up with a Stoe & Cie θ/θ powder diffractometer. For this purpose the sintered compounds were ground and mixed with high purity Si powder (as a standard for calibration). Scanning was performed at room temperature in the diffraction angle range between $2\theta = 20°$ and 90° with a step size of 0.05°.

Magnetization measurements were performed at selected temperatures between 225 and 400 K using a homemade 69 Hz vibrating-sample magnetometer equipped with an electromagnet providing a homogeneous field of up to 1.2 T.

The zero-field heat capacity of the samples was measured using a Seiko DCS-120 differential scanning calorimetry instrument. This involved a baseline measurement with empty crucibles, a reference measurement with a specimen with known specific heat (in this case Ag) and a sample measurement. The heat capacity, C_P, of the sample was then deduced from the expression

$$C_P = \frac{\Phi_{ref} - \Phi_{base}}{\Phi_{sample} - \Phi_{base}} \frac{m_{ref}}{m_{sample}} C_{P,ref}, \tag{9}$$

where Φ_{base}, Φ_{ref}, Φ_{sample} are heat flows obtained for the empty sample holders, the reference, and the sample, respectively, m_{ref} and m_{sample} are the mass of the reference specimen and the sample, respectively, and $C_{P,ref}$ is the specific heat of the reference material. Measurements were carried out between 225 and 400 K with a heating rate of 2 K min^{-1}.

Direct measurements of the magnetocaloric effect were performed as follows. The LCSM sample was placed in a container made of Teflon®. A NiCr–Ni thermocouple was mounted in direct contact with the sample and the temperature was monitored continuously using a digital voltmeter. The influence of the magnetic field on the thermocouple voltage was tested in advance and was found to be negligible. The sample container was placed in a liquid nitrogen

cooled cryostat supplied with a differential temperature controlling system. The sample could be moved manually in and out of the pole gap of an electromagnet providing a homogeneous magnetic field of up to 0.7 T. The sample was cooled down to the initial measuring temperature (around 200 K). The temperature was then increased at a rate of 0.5 K min^{-1}. The magnetic field was applied every 90 s and the sample was kept in the field for about 30 s, which was sufficient for the temperature to stabilize. The adiabatic temperature change was defined as the difference between sample temperatures obtained before and after applying the field. In the following we take the initial fields in both direct and indirect measurements to be 0, i.e. we neglect the Earth's magnetic field and possible stray fields of the magnet systems used for the investigation.

4. Results and discussion

X-ray diffraction data confirmed that the $La_{0.67}Ca_{0.33-x}Sr_xMnO_{3\pm\delta}$ samples were single-phase perovskites. The x-ray patterns were analysed by means of the Rietveld technique. The end members, $La_{0.67}Ca_{0.33}MnO_{3\pm\delta}$ and $La_{0.67}Sr_{0.33}MnO_{3\pm\delta}$, were found to crystallize in an orthorhombic structure ($Pbnm$) and a rhombohedral structure $La_{0.67}Sr_{0.33}MnO_{3\pm\delta}$ ($R\bar{3}c$) structure, respectively, in agreement with previous works [18, 25]. For the intermediate compositions, a transition from orthorhombic to rhombohedral symmetry took place around $x = 0.110$, although the samples with $x = 0.055$ and 0.110 could be described as being mixed phase. Figure 1 shows x-ray diffraction patterns for the LCSM series, which clearly reflect the structural changes caused by the replacement of Ca by Sr. The enlarged view of the $2\theta = 32°$–$33.5°$ range illustrates how the intense 112 reflection of the $Pbnm$ phase (which is flanked by two weaker reflections) gradually transforms into the $R\bar{3}c$ doublet (200 and 020) when the Sr content is increased. The transformation appears to be complete for $x = 0.165$.

The Rietveld analysis showed that the Mn–O bond distance was almost the same (∼0.196 nm) for all sample compositions, whereas the Mn–O–Mn bond angle increased from ∼162 to ∼170 °C with increasing Sr content. These observations are also in good agreement with previous literature [26, 27]. It is well known that there is a strong correlation between structural and magnetic properties of manganites. The oxygen ion mediates the magnetic exchange between neighbouring manganese ions, and the strength of the ferromagnetic exchange coupling therefore depends strongly on the Mn–O bond distance and on the Mn–O–Mn bond angle. The gradual increase of the Mn–O–Mn bond angle enhances the $e_g(Mn)-p_\sigma(O)-e_g(Mn)$ hybridization [27], which explains the systematic increase of the Curie temperature, T_C, from 267 to 367 K, which was observed for the $La_{0.67}Ca_{0.33-x}Sr_xMnO_{3\pm\delta}$ series when x was increased from 0 to 0.33. The observed Curie temperatures are listed in table 1. As can be seen from equations (1) and (3), the magnetocaloric effect is large when the variation of magnetization with temperature is large, i.e. near the Curie temperature. The possibility of tailoring compounds with given Curie temperatures over a wide temperature range extending both below and above room temperature by adjusting the chemical composition is therefore an important feature of the lanthanum manganites. On the basis of the structural analysis, the density of the LCSM compounds was found to vary linearly between 6040 kg m^{-3} for $x = 0$ and 6390 kg m^{-3} for $x = 0.33$: below we use these density values to calculate volumetric cooling power values, not taking into account the sample porosity.

Figure 2 shows the temperature dependence of the isothermal magnetic entropy change for the seven LCSM samples. The inset in figure 2 shows the series of isothermal magnetization curves used for calculation of the entropy change in the $x = 0$ sample. Although the maximum applied field was 1.2 T (cf the inset), the entropy changes were calculated for a field change of

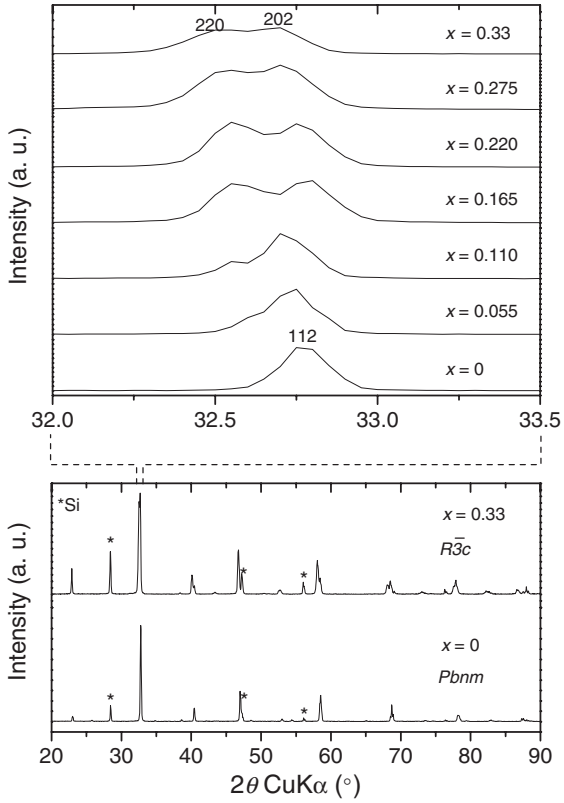

Figure 1. Bottom plate: x-ray diffraction patterns of the end members of the LCSM series mixed with Si. Top plate: enlarged view of the $2\theta = 32°$–$33.5°$ range with XRD data for all samples in the series.

Table 1. Summary of the magnetocaloric properties obtained for the $La_{0.67}Ca_{0.33-x}Sr_xMnO_{3\pm\delta}$ compounds with a field change of 1.2 T. Values for the adiabatic temperature change were calculated from combined heat capacity and magnetization data. The table shows: Curie temperatures, T_C, maximum magnetic entropy change, $|\Delta S_M(\max)|$, calculated maximum adiabatic temperature change $\Delta T_{ad}(\max)$, peak widths at half-maximum (W), and relative cooling capacities (RCP). Approximate values for gadolinium, obtained by interpolation of data presented in [21], are shown for comparison.

Sample	T_C	$\lvert\Delta S_M(\max)\rvert$		$W(\Delta S_M)$	RCP(S)	$\Delta T_{ad}(\max)$	$W(\Delta T_{ad})$	RCP(T)
x	(K)	(J kg^{-1} K^{-1})	(mJ cm^{-3} K^{-1})	(K)	(mJ cm^{-3})	(K)	(K)	(K^2)
0	267	5.9	35.6	8.5	303	2.0	9	18
0.055	285	2.8	17.1	18	307	1.0	22	22
0.110	309	2.6	16.0	21	336	n/a	n/a	n/a
0.165	332	1.8	11.2	30	336	0.93	31	29
0.220	344	1.6	10.0	33	331	0.88	33	29
0.275	353	1.5	9.5	29	276	0.80	33	26
0.33	369	1.8	11.5	28	322	1.07	27	29
Gd	293	3.3	26.1	36	940	4.2	25	105

0.7 T to allow comparison with the $\Delta T_{ad}(T)_{\Delta H}$ measurements presented below. The LCSM compounds show typical caret-shaped magnetocaloric peaks centred in the vicinity of their

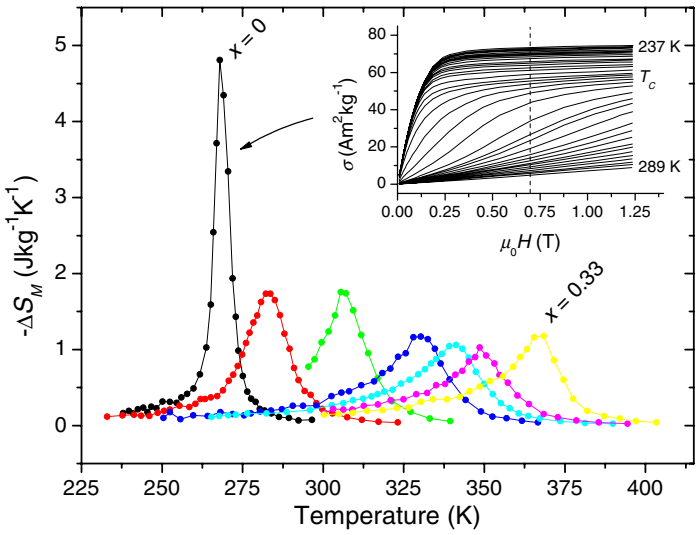

Figure 2. Temperature dependence of the isothermal magnetic entropy change for the LCSM compounds given for $\mu_0\Delta H = 0.7$ T. The inset shows the series of isothermal magnetization curves used for the calculation of the entropy change in the $x = 0$ sample. The dashed line indicates the integration maximum.

Curie temperatures. What immediately catches attention is the very sharp peak obtained for the sample containing no Sr ($x = 0$). The maximum magnetic entropy change is approximately 5 J kg^{-1} K^{-1}, which is quite high considering the rather modest field change. However, the peak is centred far below room temperature (at ∼267 K) and the temperature working range, i.e. the width of the $\Delta S_{\mathrm{M}}(T)_{\Delta H}$ peak, is quite narrow (about 5.6 K). Both the maximum value and the peak width could of course be extended by applying a larger magnetic field. The remaining samples in the series show a smaller magnetocaloric effect with a maximum of about 1.5 J kg^{-1} K^{-1}. The effect decreases when the Sr content is increased. On the other hand, the magnetocaloric peaks become broader, so the temperature working range is enhanced. In fact, the relative cooling power, RCP(S), which depends both on the height and the width of the magnetocaloric peaks, cf equation (4), is almost constant (∼160–175 mJ cm^{-3}) over the entire LCSM series. The maximum entropy changes and the relative cooling powers obtained for a field change of 1.2 T are listed in table 1.

Figure 3 shows an example of the temperature profile obtained under a direct measurement of the adiabatic temperature change, in this case for a measurement performed with the $La_{0.67}Ca_{0.33}MnO_{3\pm\delta}$ sample. Each of the step-like features on the curve corresponds to a magnetization–demagnetization sequence, where the sample temperature increases upon application of the external field (0.7 T) and subsequently decreases when the field is removed. The magnetocaloric response clearly increases as the sample temperature approaches the Curie temperature (267 K). Above T_{C} the effect gradually vanishes. The inset in figure 3 shows an enlarged view of a single magnetization cycle and illustrates how the data were used to extract the adiabatic temperature change. Analysing the successive magnetization cycles in this way, the temperature dependence of adiabatic temperature change was obtained.

Figure 4 shows $\Delta T_{\mathrm{ad}}(T)_{\Delta H}$ curves for the entire LCSM series obtained with a field change of 0.7 T. For practical reasons measurements could not be performed above 360 K, which explains why the curves are cut off at this temperature. As in the case of the magnetic entropy change, the $\Delta T_{\mathrm{ad}}(T)_{\Delta H}$ peaks are caret shaped and they are centred near the Curie temperature.

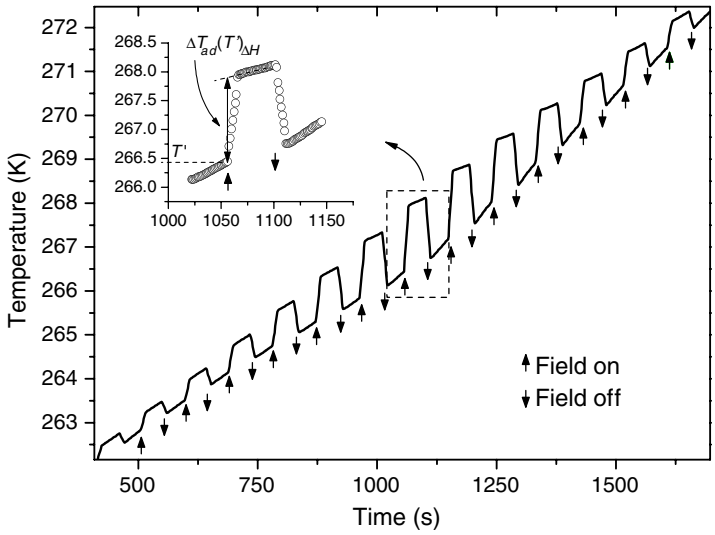

Figure 3. Temperature profile obtained under a direct measurement of the adiabatic temperature change in $La_{0.67}Ca_{0.33}MnO_{3\pm\delta}$. Arrows pointing up and arrows pointing down, respectively, indicate the application and removal of the magnetic field. The inset shows an enlarged view of a single magnetization cycle and indicates how the adiabatic temperature change was deduced.

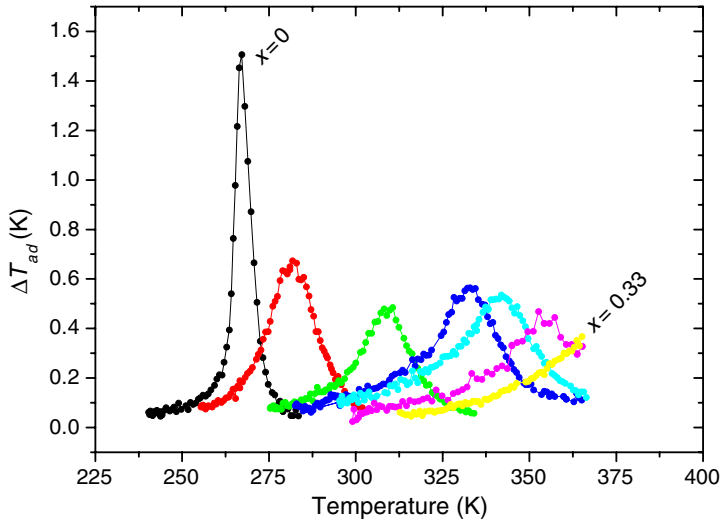

Figure 4. Temperature dependence of the adiabatic temperature change of the LCSM samples. The magnetic field change was 0.7 T.

The $La_{0.67}Ca_{0.33}MnO_{3\pm\delta}$ sample shows a maximum adiabatic temperature change of about 1.5 K. The maximum $\Delta T_{\rm ad}(T)_{\Delta H}$ value is lower for the compounds with $x > 0$. Similarly to the magnetic entropy change, the intense but narrow magnetocaloric peak obtained for the $x = 0$ sample gives almost the same relative cooling power, $\mathrm{RCP}(T) \approx 10\ \mathrm{K}^2$, as the less intense but much wider peaks obtained for the remaining samples. The comparatively low temperature change obtained for the $x = 0.110$ compound could be due to poor thermal contact between the sample and the thermocouple in this case.

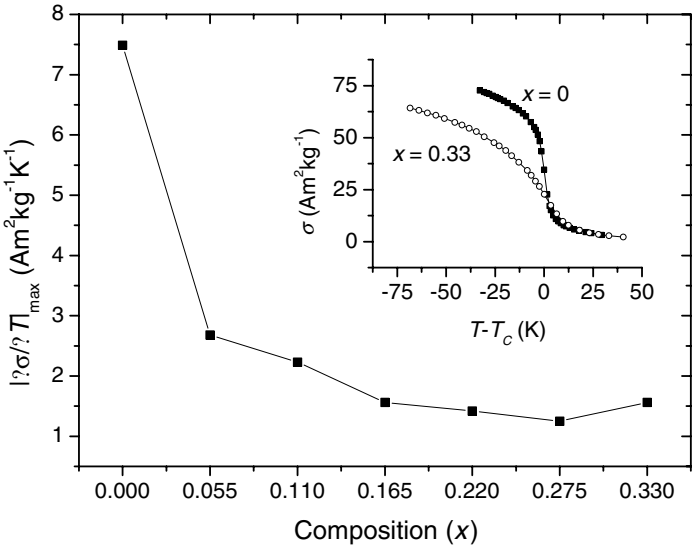

Figure 5. Maximum slope of a magnetization curve obtained in an external field of 0.25 T as a function of composition (given by x). The inset shows the constant-field magnetization curves for the two end members of the LSCM series (plotted relative to the Curie temperature).

The marked difference between the magnetocaloric response of the sample containing no Sr and the remaining samples is probably due to a difference in the nature of the ferromagnetic-to-paramagnetic transition. Figure 5 shows the magnitude of the maximum slope of the magnetization curves obtained in a constant field of 0.25 T plotted against the composition parameter x. The graph shows that the magnetic phase transition is much sharper in the $La_{0.67}Ca_{0.33}MnO_{3\pm\delta}$ compound than it is in the samples with $x > 0$ (see also the inset). As previously suggested (see e.g. [18, 28]), the reason for the difference is most probably that the ferromagnetic transition in the orthorhombic $x = 0$ sample is accompanied by an abrupt change of the lattice parameters, caused by the dynamic Jahn–Teller effect. The volume change contributes to the change of magnetization, and the magnetic transition becomes sharper. The rhombohedral ($R\bar{3}c$) symmetry does not facilitate the splitting of the e_g orbital, and accordingly less sharp ferromagnetic-to-paramagnetic transitions and smaller magnetocaloric effects are observed for the samples with $x > 0$. However, from the magnetic entropy change the compounds with $x = 0.055$ and 0.110 appear to show an intermediate behaviour, which might be expected from the XRD data; cf figure 1.

Figure 6 shows the temperature dependence of the zero-field heat capacity of the LCSM samples. For all the samples C_P increases to a point just below the Curie temperature and then shows a rather sharp drop to a level of around 520 J kg^{-1} K^{-1}. The peaks in the heat capacity curves at the Curie temperature superimpose on the lattice and electronic heat capacities. As expected from the considerations above, the $La_{0.67}Ca_{0.33}MnO_{3\pm\delta}$ sample shows the most distinct heat capacity peak. Due to difficulties of switching from cooling below room temperature to heating above room temperature, the $x = 0.110$ sample was only characterized above room temperature. However, the available data are sufficient to reveal the expected behaviour near the Curie temperature.

As outlined in section 2, the zero-field heat capacity data could be used to make a quantitative comparison between the direct and indirect measurements of the magnetocaloric effect in the LCSM system presented above. Figure 7 shows an example of an entropy–

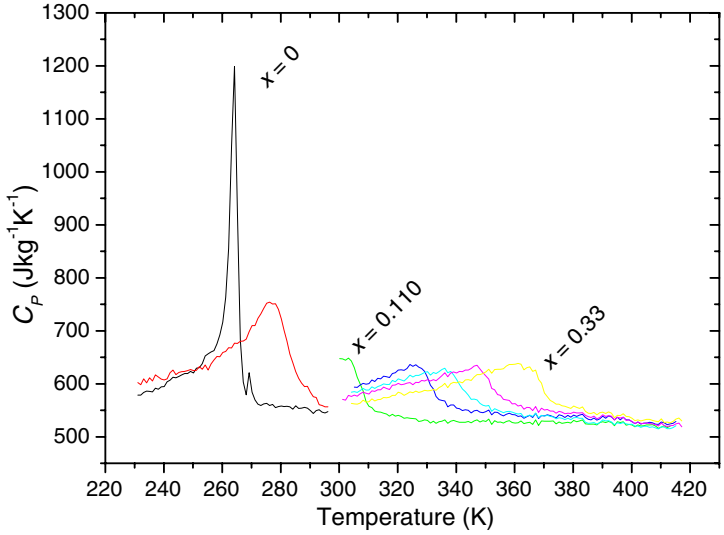

Figure 6. Zero-field heat capacity as a function of temperature for the LCSM samples. Below room temperature data for the $x = 0.110$ sample are missing.

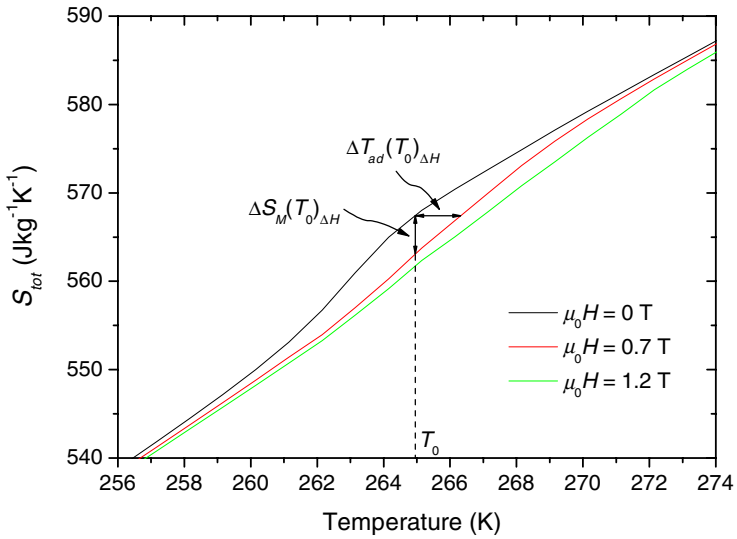

Figure 7. Entropy–temperature diagram calculated from the measured isothermal magnetic entropy change and the zero-field heat capacity and for $La_{0.67}Ca_{0.33}MnO_{3\pm\delta}$ with isofield curves for $\mu_0 H = 0$, 0.7, and 1.2 T. The determination of the adiabatic temperature change due to a field change of 0.7 T at a given temperature T_0 is illustrated.

temperature diagram generated from the combined zero-field heat capacity and magnetization measured, in this case for the $La_{0.67}Ca_{0.33}MnO_{3\pm\delta}$ compound. The diagram shows isofield lines for $\mu_0 H = 0$, 0.7, and 1.2 T. The S–T diagram is interesting form a technological viewpoint because it can be used to evaluate the performance of the material in different magnetic cooling cycles. Here it was used to extract values for the adiabatic temperature change due to a field change of 0.7 T, which could then be compared with the experimentally observed values.

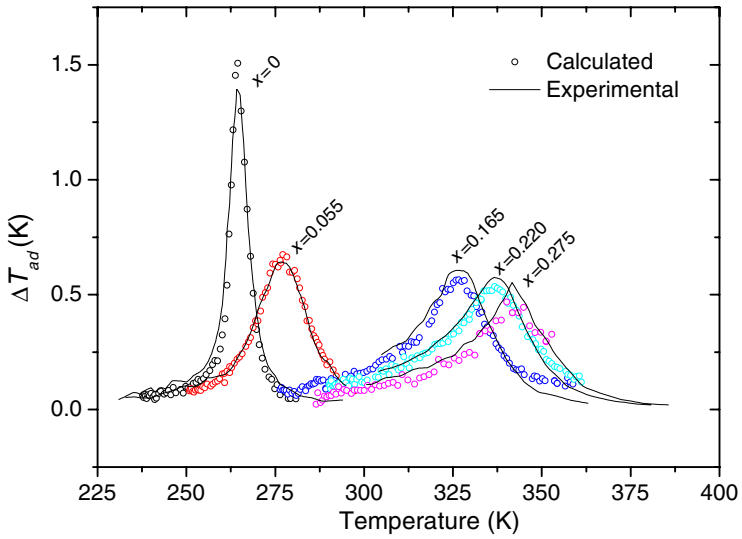

Figure 8. Comparison between calculated and measured adiabatic temperature changes (full lines and circles, respectively) obtained with a field change of 0.7 T (selected LCSM compounds only).

Figure 8 compares calculated and measured adiabatic temperature changes for selected LCSM samples (the $x = 0.110$ and 0.33 compounds were excluded due to the lack of heat capacity and temperature data, respectively). It should be mentioned that the experimental $\Delta T_{\rm ad}(T)_{\Delta H}$ curves were shifted slightly (2–5 K) on the temperature axis to make the peak maxima between calculated and observed data coincide. Except for the discrepancy in peak positions, which we ascribe to thermocouple offsets, there is an excellent agreement between the calculated and the measured temperature profiles. After in this way having validated the consistency between the direct and indirect measurements of the magnetocaloric effect in the LCSM series, the S–T diagrams were used to predict adiabatic temperature changes for a field change of 1.2 T, which is probably more relevant from a technological viewpoint. Table 1 summarizes the results on the magnetocaloric effect for the entire LCSM series and compares the magnetocaloric quantities with those reported for gadolinium (values for Gd were obtained from [21] using a linear interpolation between data given for field changes of 1 and 2 T).

In the table the maximum magnetic entropy change is shown both per unit mass (as in figures 4 and 7) and per unit volume. The volumetric values of $\Delta S_{\rm M}(T)_{\Delta H}$ are important because the actual size of the magnetic refrigerant strongly influences the cost of the magnet system used to provide the magnetic field in a cooling device [19]. The magnetic entropy changes per unit mass obtained for the LCSM compounds are comparable to that for gadolinium, especially for the samples with low Sr content and in particular for the $x = 0$ sample, which shows a larger maximum value. However, if the temperature working range, i.e. the width of the $\Delta S_{\rm M}(T)_{\Delta H}$ peaks, and the difference in density are taken into account it becomes clear that Gd provides a higher cooling power than the manganites. The LCSM compounds show a relative cooling power based on the entropy change, RCP(S), of about 275–335 mJ cm^{-3}. The RCP(S) value for Gd is approximately three times larger. The picture is quite similar considering the adiabatic temperature change, where the relative cooling power of Gd exceeds that of LCSM by a factor of 3–5. Basically this means that in order to obtain an equivalent cooling capacity a refrigerant unit consisting of LCSM must have at least three times the volume of a refrigerant unit consisting of Gd. However, LCSM compounds are

applicable at temperatures well above 300 K, where the cooling power of Gd is negligible. Moreover, manganites may provide lower production cost and improved durability. The latter could be the case due to the high chemical stability of the oxides.

It has been shown [2] that the performance of active magnetic regenerative refrigerators can be enhanced if the magnetocaloric effect of the refrigerant unit varies in accordance with the temperature gradient between the cold end and the hot end of the device, such that each segment of the refrigerant operates near its magnetocaloric optimum. As we have shown above, $La_{0.67}Ca_{0.33-x}Sr_xMnO_{3\pm\delta}$ compounds with a low Sr content exhibit a reasonable magnetocaloric effect and it is possible to precisely control the Curie temperature. LCSM compounds might therefore have potential as working materials in multi-component refrigerant units, where they could be included to cover specific temperature regions. It should be mentioned that the Curie temperature of Gd can also be varied (below 293 K) by alloying it with for instance Dy [30].

5. Conclusions

The magnetocaloric properties of a series of lanthanum manganites, $La_{0.67}Ca_{0.33-x}Sr_xMnO_{3\pm\delta}$ with $x \in [0; 0.33]$ have been investigated. The isothermal magnetic entropy change was deduced form magnetization measurements performed between 0 and 1.2 T. The adiabatic temperature change was measured directly under a field change of 0.7 T. On the basis of zero-field heat capacity measurements and the indirectly measured $\Delta S_M(T)_{\Delta H}$, the temperature dependence of the adiabatic temperature change upon a field change of 0.7 T was calculated. An excellent agreement between calculated and experimental $\Delta T_{ad}(T)_{\Delta H}$ profiles was obtained, which can be taken as a validation of the consistency between the two kinds of measuring techniques. The magnetocaloric effect in the orthorhombic $La_{0.67}Ca_{0.33}MnO_{3\pm\delta}$ compound was significantly higher than that of the remaining compounds. We ascribe this to the dynamic Jahn–Teller effect, which has previously been shown to cause an abrupt volume change near the ferromagnetic transition temperature in LCSM compounds with an orthorhombic crystallographic structure. The volume change contributes to the change of magnetization and leads to an enhanced magnetocaloric effect. The dynamic Jahn–Teller effect is absent in the compounds with $x > 0$, which are rhombohedral, although the samples with $x = 0.055$ and 0.110 are probably mixed phase and show an intermediate behaviour. The magnetocaloric properties of the LCSM compounds were compared to those of gadolinium, which is considered a prototype material for magnetic refrigeration near room temperature. The relative cooling power of the LCSM compounds was found to be about three times lower than that of Gd. However, the $La_{0.67}Ca_{0.33-x}Sr_xMnO_{3\pm\delta}$ compounds that we have studied can be tailored to have Curie temperatures between 267 and 369 K. Therefore, they could have technological application in multi-component refrigerant units for cooling over a wide temperature range.

Acknowledgments

The work was in part supported by the Danish Technical Research Council. Dr Claus Schelde Jacobsen is acknowledged for assisting in the experimental work.

References

[1] Gschneidner K A Jr and Pecharsky V K 2000 *Annu. Rev. Mater. Sci.* **30** 387
[2] Hirano N, Nagaya S, Takahashi M, Kuriyama T, Ito K and Nomura S 2002 *Adv. Cryog. Eng.: Proc. Cryog. Eng. Conf.* **47** 1027

[3] Clot P, Viallet D, Allab F, Kedous-Lebouc A, Fournier J M and Yonnet J 2003 *IEEE Trans. Magn.* **39** 3349
[4] Richard M-A, Rowe A M and Chahinea R 2004 *J. Appl. Phys.* **95** 2146
[5] Brown G V 1976 *J. Appl. Phys.* **47** 3673
[6] Pecharsky V K and Gschneidner K A Jr 1997 *Phys. Rev. Lett.* **78** 4494
[7] Brück E, Tegus O, Zhang L, Li X W, de Boer F R and Buschow K H J 2004 *J. Alloys Compounds* **383** 32
[8] Hu F-X, Shen B-G, Sun J-R, Chen Z-H and Zhang X-X 2000 *J. Phys.: Condens. Matter* **12** L691
[9] Morelli D T, Mance A M, Mantese J V and Micheli A L 1996 *J. Appl. Phys.* **79** 373
[10] Wang Z M, Ni G, Xu Q Y, Sang H and Du Y W 2001 *J. Appl. Phys.* **90** 5689
[11] Zhang X X, Tejada J, Xin Y, Sun G F, Wong K W and Bohigas X 1996 *Appl. Phys. Lett.* **69** 3596
[12] Guo Z B, Yang W, Shen Y T and Du Y W *Solid State Commun.* **105** 89
[13] Sun Y, Tong W and Zhang Y 2001 *J. Magn. Magn. Mater.* **232** 205
[14] Zhong W, Chen W, Ding W, Zhang N, Hu A, Du Y W and Yan Q J 1998 *Eur. Phys. J.* B **3** 169
[15] Bose T K, Chahine R, Gopal B R, Foldeaki M, Barman A, Gosh M, De B R and Chatterjee S 1998 *Cryogenics* **38** 849
[16] Bohigas X, Tejada J, Marínez-Sarrión M L, Tripp S and Black R 2000 *J. Magn. Magn. Mater.* **208** 85
[17] Dinesen A R, Linderoth S and Mørup S 2002 *J. Magn. Magn. Mater.* **253** 28
[18] Mira J, Rivas J, Hueso L E, Rivadulla F and Quintela M A L 2002 *J. Appl. Phys.* **91** 8903
[19] Pecharsky V K and Gschneidner K A Jr 2001 *J. Appl. Phys.* **90** 4614
[20] Pecharsky V K and Gschneidner K A Jr 1999 *J. Appl. Phys.* **86** 565
[21] Lee J S 2004 *Phys. Status Solidi* b **241** 1765
[22] Ghivelder L, Abrego Castillo I, Alford N McN, Tomka G J, Riedi P C, MacManus-Driscoll J, Akther Hossain A K M and Cohen L F 1998 *J. Magn. Magn. Mater.* **189** 274
[23] Woodfield B F, Wilson M L and Byers J M 1997 *Phys. Rev. Lett.* **78** 3201
[24] Chick L A, Pederson L R, Manpin G D, Bates J F, Thomas L E and Exarthos G J 1990 *Mater. Lett.* **10** 6
[25] Guo Y Q, Zhang X H and Wappling R 2000 *J. Alloys Compounds* **306** 133
[26] García-Muñoz J L, Fontcuberta J, Martínez B, Seffar A, Piñol S and Obradors X 1997 *Phys. Rev.* B **55** R668
[27] García-Muñoz J L, Fontcuberta J, Suaaidi M and Obradors X 1996 *J. Phys.: Condens. Matter* **8** L787
[28] Dai P, Zhang J, Mook H A, Liou S-H, Dowben A and Plummer E W 1996 *Phys. Rev.* B **54** R3694
[29] Rowe A M and Barclay J A 2003 *J. Appl. Phys.* **93** 1672
[30] Smaïli A and Chahine R 1997 *J. Appl. Phys.* **81** 824